

RESEARCH

Open Access



# Simple and rapid colorimetric sensing of Ni(II) ions in tap water based on aggregation of citrate-stabilized silver nanoparticles

Francis Eric P. Almaquer<sup>\*</sup> , John Salvador Y. Ricacho and Ryan Lee G. Ronquillo

## Abstract

The presence of nickel in our water sources presents a danger to human health and aquatic organisms alike. Therefore, there is a need to detect and monitor nickel concentration in these sources. Current detection methods use instruments that are costly, resource intensive and require skilled personnel. Alternative methods that are simple and fast are needed. This study reports for the first time the development of a simple colorimetric assay for the detection of Ni<sup>2+</sup> in aqueous solution using citrate-stabilized silver nanoparticles. Chemical synthesis method was employed using sodium borohydride and trisodium citrate as reducing and stabilizing agents, respectively. The characterization techniques used for obtaining spectral and morphological properties were ultraviolet-visible spectroscopy and transmission electron microscopy. The resultant silver nanoparticle solution was yellow in color and exhibited an absorbance peak at 392 nm. The full width at half maximum value was  $57.8 \pm 1.3$  nm indicating particle monodispersity. For the morphology, the nanoparticles were spherical in shape with an average size of  $10.4 \pm 4.5$  nm. Furthermore, the colorimetric properties of the silver nanoparticles for Ni<sup>2+</sup> detection was investigated. Ni<sup>2+</sup> was visually detected through a fast solution color change from yellow to orange. Monitoring of the absorbance showed a decrease in the original 392 nm peak and broadening of the surface plasmon absorption band. These changes are attributed to the aggregation of the nanoparticles due to Ni<sup>2+</sup> addition which was confirmed by the transmission electron microscopy imaging. The absorption ratio ( $A_{510}/A_{392}$ ) was plotted against varying Ni<sup>2+</sup> concentration and it exhibited a good linear correlation from 0.7 to 1.6 mM with an R<sup>2</sup> of 0.9958. The limits of detection and quantification were 0.75 and 1.52 mM, respectively. Additionally, the assay was tested against other common ions and showed excellent selectivity for Ni<sup>2+</sup>. Finally, the assay was successfully tested to detect Ni<sup>2+</sup> in tap water samples with an average difference of 16% from prepared concentrations. Overall, the study showed the potential of using citrate-stabilized silver nanoparticles as a colorimetric reagent for detecting Ni<sup>2+</sup> in aqueous solution.

**Keywords:** Nanotechnology, Nanosensors, Silver nanoparticles, Nickel detection

\* Correspondence: [fpalmaquer@up.edu.ph](mailto:fpalmaquer@up.edu.ph)  
School of Technology, University of the Philippines Visayas, Miagao 5023,  
Philippines



## Introduction

Nickel is a naturally-occurring element in the environment that can be extracted from ores through mining. In recent years, the demand for nickel has increased resulting in a significant rise in global nickel production. Based on the report of Nakajima et al. [1], countries rich in nickel reserves, such as Indonesia and the Philippines, have seen increase in mining activity since the late 1990s. Inevitably, due to the increased mining activity, nickel reaches aquatic environments through spillage, dam seepage, and direct discharge. In the human body, nickel at high concentration can cause lung, brain and kidney damage among many others. Long-term exposure can also lead to muscular damage and neurological disorders as discussed by Jaishankar et al. [2]. Therefore, there is a need to detect and monitor nickel contamination levels especially in waters nearest to humans and food sources.

Current detection methods for heavy metals involve the use of sophisticated techniques such as those described by Helaluddin et al. [3] which include atomic absorption spectrometry, atomic fluorescence spectroscopy, and inductively coupled plasma optical emission spectroscopy, among others. However, these techniques are often time-consuming, resource intensive, require high capital cost and trained analysts. Hence, there is a need to explore other methods that are fast, simple and easy to use.

The development of sensors using nanotechnology is an attractive alternative because of its simplicity and viability for on-site applications. Typically, noble metal particles such as gold and silver nanoparticles are synthesized in aqueous solution and used as chemical nanosensors for various analytes. Lee et al. [4] discussed that between the two, silver nanoparticles have higher extinction coefficient and sharper extinction bands. Silver precursor metals also have lower cost compared to gold and are easier to synthesize.

Vilela et al. [5] explained the general mechanism of how nanoparticles can be used as a colorimetric sensor. Silver nanoparticle-based sensors work via colorimetry by exploiting a property called localized surface plasmon resonance, a phenomenon where the free electrons in the conduction band of the metal nanoparticles oscillate upon interaction with light. Due to this phenomenon, the silver nanoparticle solution exhibits a unique color dependent on its morphology. When the target analyte interacts with the solution, interparticle linking induces aggregation resulting in a change in the morphological state from dispersed to aggregated. Consequently, this results in a change in solution color which can then be detected by the naked eye.

In literature, silver nanoparticles have been functionalized in a variety of ways and used to detect different

heavy metals. Nsengiyuma et al. [6] have used functionalized silver nanoparticles to detect copper ions. Shrivastava et al. [7] also reported that they can be employed as sensor for chromium in various aqueous solutions and vegetable samples. Lee et al. [4] concluded that label-free silver nanoparticles can be used in the detection of zinc ions. Finally, He and Zhang [8] and Jarujamrus et al. [9] also reported of the capability of unmodified silver nanoparticles as sensors for manganese and mercury, respectively. However, some studies use potentially toxic reagents and numerous instruments in reducing, stabilizing and functionalizing the silver nanoparticles. Some also require post-synthesis modification involving high power energy-intensive equipment. For the detection of  $\text{Ni}^{2+}$ , there are limited studies available regarding the use of silver nanoparticles. Current studies have employed different chemical reagents to stabilize and functionalize the silver nanoparticles for  $\text{Ni}^{2+}$  detection such as those reported by Li et al. [10] and Shang et al. [11]. However, aside from using less commonly available reagents, the synthesis method involved time-consuming processes requiring long hours of stirring time to ensure assemblage of functionalizing agents with the nanoparticle. There is also limited study regarding the application to real water. The use of readily available nontoxic stabilizing agents that require simpler synthesis method is sought.

In this study, the development of a silver nanoparticle assay for  $\text{Ni}^{2+}$  sensing that uses trisodium citrate as a commonly available reagent and environmentally benign stabilizer is reported for the first time. The synthesis method with citrate is also simplified. There is also no further need for post-synthesis modifications. The colorimetric performance of the citrate-stabilized silver nanoparticles for  $\text{Ni}^{2+}$  detection was evaluated by investigating resultant changes in color, absorbance behavior and morphology. Selectivity test over other common ions was also conducted to ensure preference for  $\text{Ni}^{2+}$ . Finally, to extend application to real water samples, it was used to detect  $\text{Ni}^{2+}$  in tap water.

## Materials and methods

### Chemicals and instruments

The following chemicals were used in the experiments: silver nitrate (99.9% Silver nitrate ( $\text{AgNO}_3$ ), Loba Chemie, Mumbai, India), sodium borohydride (97% sodium borohydride ( $\text{NaBH}_4$ ), Loba Chemie, Mumbai, India), trisodium citrate dihydrate (99%  $\text{Na}_3\text{C}_6\text{H}_5\text{O}_7 \cdot 2\text{H}_2\text{O}$ , Loba Chemie, Mumbai, India), nickel sulfate ( $\geq 96\%$   $\text{NiSO}_4$ , Ajax FineChem), calcium chloride ( $\geq 96\%$   $\text{CaCl}_2$ , Sigma-Aldrich), magnesium sulfate heptahydrate ( $\geq 98\%$   $\text{MgSO}_4 \cdot 7\text{H}_2\text{O}$ , Ajax FineChem) and lithium chloride (99%  $\text{LiCl}$ , Techno PharmChem). Ultraviolet-visible (UV-Vis) absorbance spectra were determined using Thermo Scientific GENESYS

10S UV-Vis Spectrophotometer. The morphology and size of the nanoparticles were characterized using JEOL JEM 1010 transmission electron microscope (TEM) from Peabody, MA. All aqueous solutions were prepared with distilled water unless otherwise stated. All glasswares were thoroughly cleaned and rinsed prior to use.

#### Synthesis of citrate-stabilized silver nanoparticles

Colloidal citrate-stabilized silver nanoparticles were synthesized using the modified Creighton method [12].  $\text{AgNO}_3$ ,  $\text{NaBH}_4$  and trisodium citrate dihydrate ( $\text{Na}_3\text{C}_6\text{H}_5\text{O}_7 \cdot 2\text{H}_2\text{O}$ ) were used as precursor metal, reducing agent and stabilizing agent, respectively. Initially, 30 mL of 2 mM cold  $\text{NaBH}_4$  solution was placed inside a 250 mL Erlenmeyer flask together with a magnetic stir bar. The flask was then placed in an ice bath mounted on a stir plate. Under continued stirring at 450 rpm, 10 mL of 1 mM  $\text{AgNO}_3$  was added dropwise. After adding all the  $\text{AgNO}_3$ , 5 mL of 1 mM trisodium citrate dihydrate solution was added in the same manner. The stirring was stopped when all the citrate has been added. The citrate-stabilized silver nanoparticle solution was stored at room conditions for 1 h prior to use.

#### Characterization of citrate-stabilized silver nanoparticles

The absorbance spectra of the citrate-stabilized silver nanoparticles were recorded using a UV-Vis spectrophotometer. Cuvettes of 1.5 mL volume capacity and 10 mm path lengths were used in the study. Absorbance was read from 350 to 700 nm wavelength for each sample. To analyze the morphology, samples were sent to the Southeast Asian Fisheries Development Center in Tigbauan, Iloilo, Philippines. TEM was employed to reveal the size and morphological properties of the silver nanoparticles. A sample was prepared by drying a small drop of freshly synthesized citrate-stabilized silver nanoparticle solution on a Formvar-coated 200-mesh copper grid. The sample was then mounted on the JEOL JEM-1010 TEM and a 100-kV electron beam passed through the sample.

#### Nickel sensing experiment

$\text{Ni}^{2+}$  solutions of different concentrations from 0.6 to 1.6 mM were prepared. Then, 3 mL of the citrate-stabilized silver nanoparticle solution was transferred to a 5-mL glass vial. Afterwards, 0.5 mL of the  $\text{Ni}^{2+}$  solution was added to the glass vial containing the nanoparticle solution. The effects of the varying  $\text{Ni}^{2+}$  concentrations were evaluated by investigating the changes in color, absorbance curve behavior, and morphology. A calibration curve was then generated to determine the relationship between the absorbance behavior and  $\text{Ni}^{2+}$  concentration. The limits of detection

and quantification were then calculated using the linear regression method discussed by Sanagi et al. [13].

#### Selectivity tests

The following ions were used in the selectivity test:  $\text{Ca}^{2+}$  from  $\text{CaCl}_2$ ,  $\text{Mg}^{2+}$  from  $\text{MgSO}_4 \cdot 7\text{H}_2\text{O}$ ,  $\text{Ag}^+$  from  $\text{AgNO}_3$ ,  $\text{Li}^+$  from  $\text{LiCl}$ , and  $\text{Ni}^{2+}$  from  $\text{NiSO}_4$ . Initially, 0.5 mL of the different metal cation solutions at 1 mM were separately added to 3 mL of the synthesized citrate-stabilized silver nanoparticles for a final cation concentration of 0.14 mM. The resultant solutions were then tested for absorbance from 350 to 700 nm using a UV-Vis spectrophotometer. Photos were also taken to observe the color changes after the addition of the metal cation solutions.

#### Nickel sensing in tap water

The tap water from the School of Technology, University of the Philippines Visayas in Iloilo, Philippines was used in the experiment. The tap water was analyzed for initial nickel concentration using a Flame Atomic Absorption Spectrophotometer (FAAS), Varian 55B. No nickel was detected by the FAAS in the tap water samples. Therefore, in the nickel sensing, tap water samples spiked with  $\text{Ni}^{2+}$  ions were used.

Three  $\text{Ni}^{2+}$  concentrations (1.1, 1.2, and 1.6 mM) were prepared using tap water. Initially, 0.5 mL of the nickel-contaminated tap water was added to 3 mL of the citrate-stabilized silver nanoparticle solution. The resultant solutions were then tested for absorbance from 350 to 700 nm using a UV-Vis spectrophotometer. Photos were also taken to observe the color changes after the addition of the contaminated tap water.

## Results and discussion

#### Characterization of citrate-stabilized silver nanoparticles

##### Optical and spectral properties

Citrate-stabilized silver nanoparticles were successfully synthesized as supported by the optical and spectral properties of the resulting solution. As shown in Fig. 1, the solution is bright yellow in color and exhibits a maximum UV-Vis absorbance peak at 392 nm.

Monodispersed citrate-stabilized silver nanoparticles exhibit yellow color in solution due to the excitation of the local surface plasmon resonance band in the UV-Vis region. Specifically, for silver nanoparticles, this plasmon resonance produces an absorption peak around 400 nm but may slightly vary depending on nanoparticle size. According to previously published works of Paramelle et al. [14] and Alula et al. [15], smaller sized nanoparticles approximately 10 nm in diameter produce a maximum absorption band around 392 nm while larger sized nanoparticles such as those 30 nm in diameter exhibit absorption peak around 406 nm.

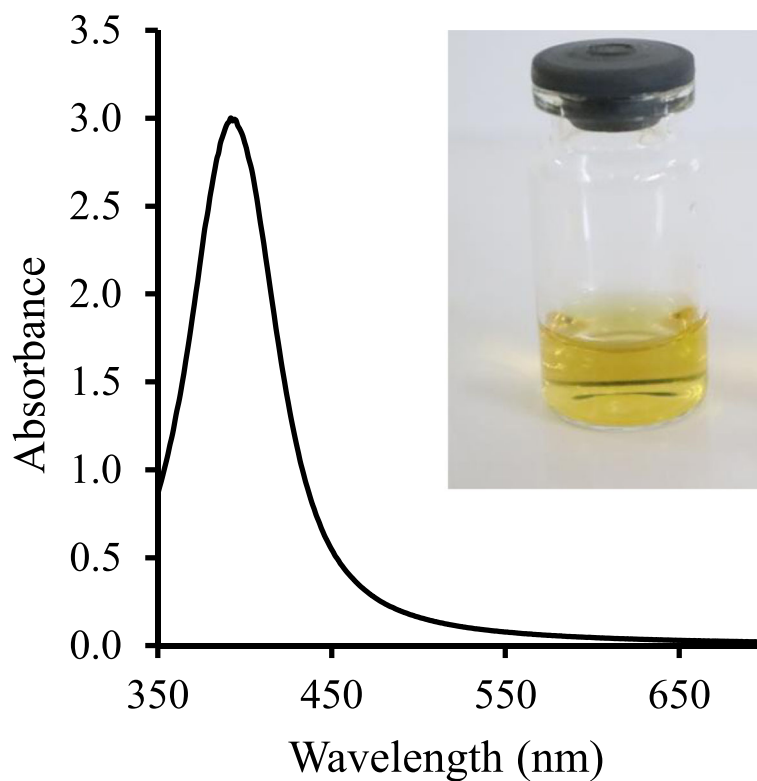


**Fig. 1** Bright yellow citrate-stabilized silver nanoparticle solution with absorbance peak at 392 nm

Additionally, other properties can be determined from the absorbance spectra of the solution. The width of the absorbance curve can be used to roughly estimate the size of the silver nanoparticles. For a monodispersed solution, nanoparticles of approximately the same size will absorb similar wavelength of light resulting to a narrow absorbance curve. For polydispersed nanoparticle solution, the particles will absorb varying wavelengths resulting in a wider curve. This can be mathematically estimated by calculating the full width at half maximum (FWHM) which is the width of the absorbance curve at half of the maximum absorbance peak. The FWHM can be analytically determined using the formula shown in Eq. (1).

$$\text{FWHM} = |\lambda_{0.5 \text{ max}} - \lambda_{\text{max}}| \times 2 \quad (1)$$

where:

$\lambda_{0.5 \text{ max}}$  = wavelength corresponding to half of the maximum absorbance.

$\lambda_{\text{max}}$  = wavelength corresponding to the maximum absorbance.

The FWHM calculated for the synthesized citrate-stabilized silver nanoparticle is  $57.8 \pm 1.3$  nm. In literature, this FWHM value corresponds to monodispersed

and uniform nanoparticle size around 10–14 nm as reported by Solomon et al. [16].

#### **Morphological properties**

Shown in Fig. 2 is the TEM image of the silver nanoparticles confirming successful synthesis of spherical nanoparticles. The average diameter is  $10.4 \pm 4.5$  nm, which is consistent with the size corresponding to the FWHM calculated earlier. The uniform size distribution and sphericity of the silver nanoparticles can be attributed to the reduction of silver nitrate with the use of sodium borohydride as a strong reducing agent as discussed by Abou El-Nour et al. [17]. The small nanoparticle sizes also result from excess borohydride used since it increases nucleation sites, reducing the sizes of particles produced.

#### **Stability**

A stabilizing agent is added to silver nanoparticles in order to prevent aggregation prior to its use in sensing applications. To evaluate the effect of trisodium citrate as a stabilizing agent, a time-lapse analysis was conducted which compared the color changes of the solutions of synthesized silver nanoparticles with citrate and without citrate.

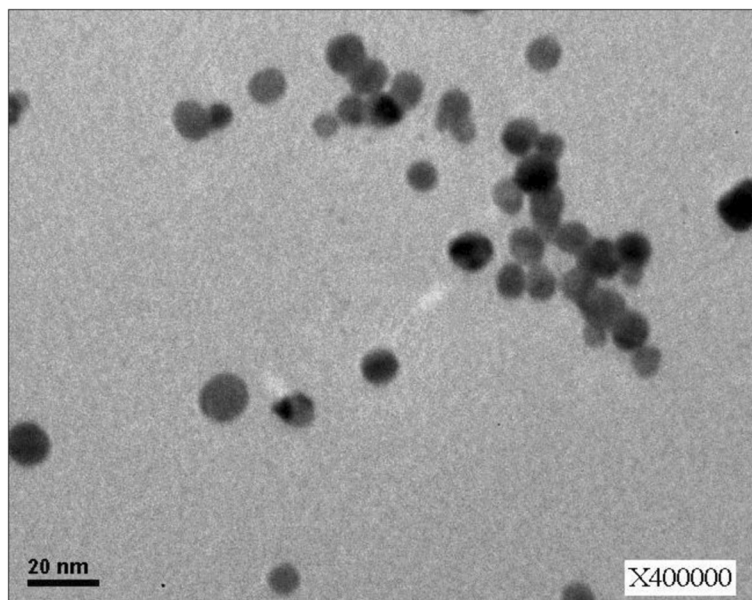


**Fig. 2** TEM image of spherical citrate-stabilized silver nanoparticles at 400,000X magnification

As shown in Fig. 3, there was eventual discoloration in solutions of silver nanoparticles without the citrate. This discoloration indicates early stages of aggregation of nanoparticles as reported by Solomon et al. [16]. This confirms that unprotected silver nanoparticles with only sodium borohydride as reducing agent is not enough to prevent particle aggregation, which is consistent with the review of Terenteva et al. [18]. This renders the solution unfit for colorimetric sensing application as it darkens immediately after synthesis. Meanwhile, silver nanoparticles with citrate retained bright yellow color for long periods of time. The stable yellow color of the nanoparticles is attributed to its non-aggregated state due to the electrostatic repulsion provided by the negative charges of the carboxyl groups of citrate present in the surface of the silver nanoparticles [19].

#### Nickel sensing

The performance of the citrate-stabilized silver nanoparticles as a colorimetric sensor for nickel as  $\text{Ni}^{2+}$  was evaluated through investigation of the various changes in the properties of the solution namely, color, absorbance spectra and morphological changes.

#### Color response

Effective colorimetric nanosensors should display fast, sharp and appreciable color change to aid in analyte detection. Upon interaction with varying concentrations of  $\text{Ni}^{2+}$ , the color of the citrate-stabilized silver nanoparticles changed from yellow to deep orange almost immediately upon addition of the heavy metal. The variation in concentrations

yielded color changes of increasing gradient from yellow to deep orange as shown in Fig. 4.

Shang et al. [11] suggested that the addition of  $\text{Ni}^{2+}$  causes the silver nanoparticles to aggregate due to the strong coordination bonds formed between  $\text{Ni}^{2+}$  ions and the carboxyl groups attached on the surface of the nanoparticles which in this case are provided by the citrate ions. The aggregation causes the visible color change of the solution from yellow to deep orange. The increasing intensity of the orange color with increasing  $\text{Ni}^{2+}$  concentrations also indicates increasing aggregation state. This color change is associated with the changes in the surface plasmon absorption band, which is dependent on particle size, shape, and distances between particles.

#### Absorbance curve response

The effect of varying  $\text{Ni}^{2+}$  concentrations on the UV-Vis absorbance curve of the citrate-stabilized silver nanoparticles was also investigated. As presented in Fig. 5, as the  $\text{Ni}^{2+}$  concentration is increased, there is reduction of absorbance value at the original 392 nm peak with eventual broadening of the surface plasmon absorption band.

The gradual decrease in absorbance value at 392 nm peak suggests an increase in size of the originally monodispersed citrate-stabilized silver nanoparticles due to aggregation [14]. Correspondingly, the widening of the plasmon absorption band indicates the transition of the solution from monodispersed to an aggregated state. This supports the earlier premise that silver nanoparticle interaction with the  $\text{Ni}^{2+}$  ions could lead to the formation of carboxyl-nickel complexes that eventually caused the particles to aggregate, thus, reducing interparticle distance [10].

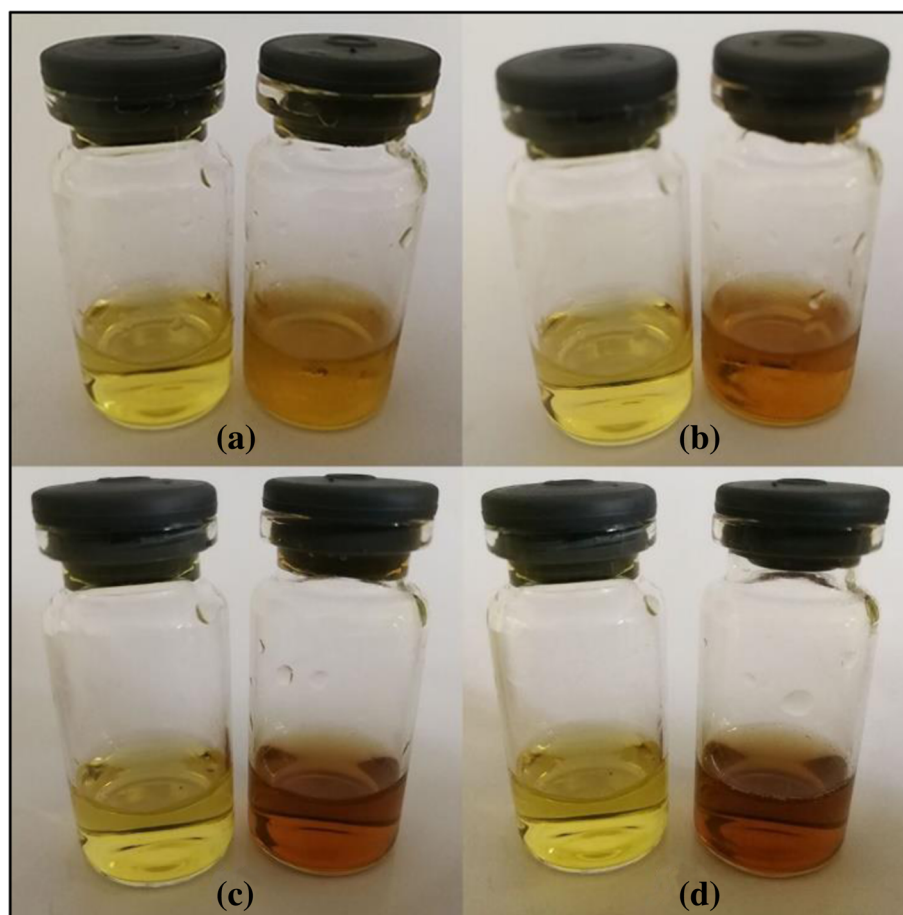


**Fig. 3** Silver nanoparticles without citrate (right panel) and with citrate (left panel) for (a) 5, (b) 10, (c) 20 and (d) 30 min

#### **Morphological response**

To confirm the aggregation behavior of the silver nanoparticles upon interaction with  $\text{Ni}^{2+}$  ions, samples with and without the heavy metal were analyzed using TEM. The  $\text{Ni}^{2+}$  concentration used in the analysis was the highest concentration used in the assay which is 1.6 mM. Figure 6 presents the TEM imaging results.

The TEM images confirm that citrate-stabilized silver nanoparticles aggregate in the presence of  $\text{Ni}^{2+}$  ions. This also confirms the cause of the color changes and absorbance curve changes exhibited by the solution.

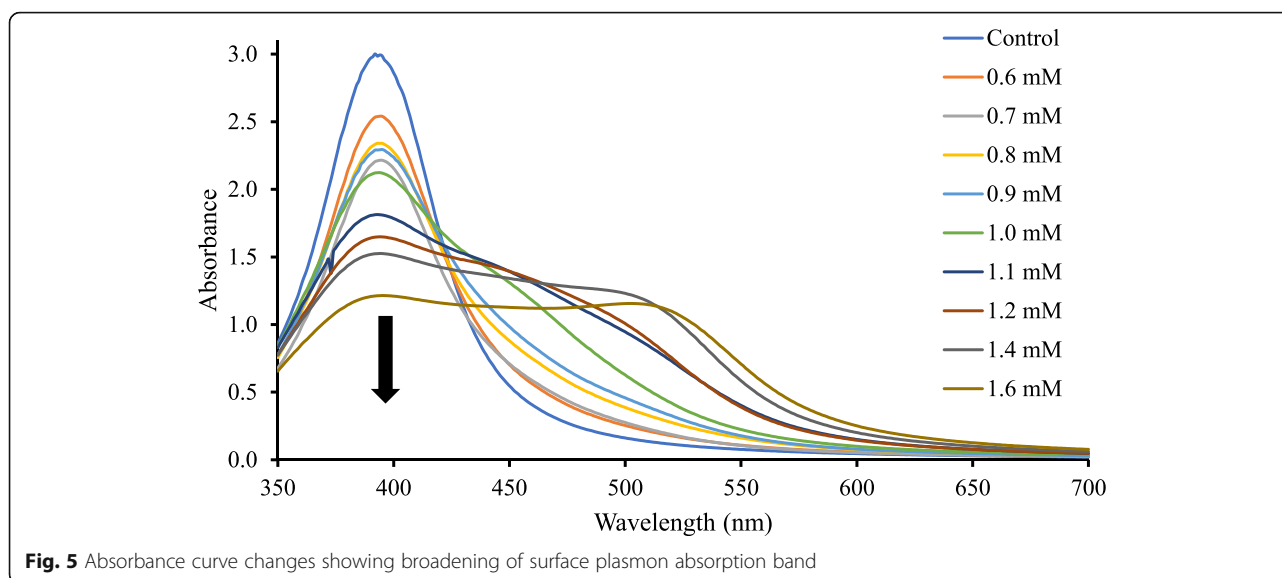
Aside from the formation of carboxyl-nickel complexes, the addition of  $\text{Ni}^{2+}$  could have reduced the negative surface charge of the silver nanoparticles thereby reducing the stability of the particles leading to aggregation [11].

#### **Proposed mechanism**

The presence of citrate ions on the surface of the silver nanoparticles provides electrostatic stability to the nanoparticle solution. This prevents the nanoparticles from prematurely aggregating keeping the solution bright



**Fig. 4** Color changes in citrate-stabilized silver nanoparticles after addition of varying  $\text{Ni}^{2+}$  concentrations (mM)



yellow as previously shown in Fig. 3. Munro et al. [20] explained the potential configuration of a citrate ion on the surface of a silver colloid. They explained that when a citrate ion bonds with a silver nanoparticle, two of the three carboxyl groups are associated with the surface of the silver nanoparticle.

However, this configuration changes when  $\text{Ni}^{2+}$  ions are introduced. Wyrzykowski and Chmurzynski [21] discussed that in the presence of  $\text{Ni}^{2+}$ , citrate ions act as a ligand and bind to the metal ion forming nickel-carboxyl complexes. During the metal binding, two carboxyl groups and a hydroxyl group participate in the formation of coordination complex with a  $\text{Ni}^{2+}$  ion. Specifically, the oxygen atoms of the two carboxyl groups and the oxygen atom of the hydroxyl group coordinate with  $\text{Ni}^{2+}$  in the process.

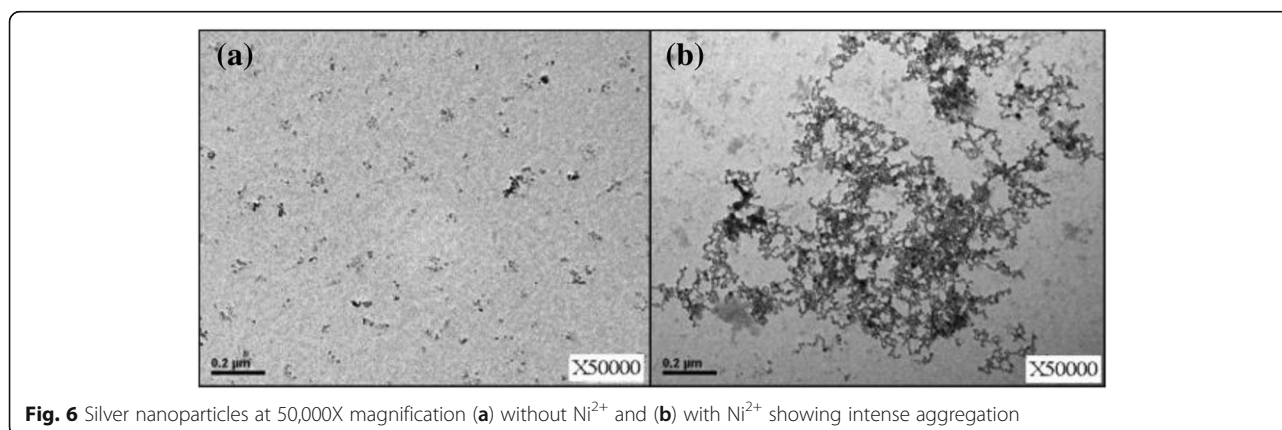
Each citrate ion has 4 potential arms for bonding, however, two of the carboxyl groups are already associated with the silver nanoparticle surface. Hence, a citrate ion can potentially coordinate with one or two  $\text{Ni}^{2+}$  ions

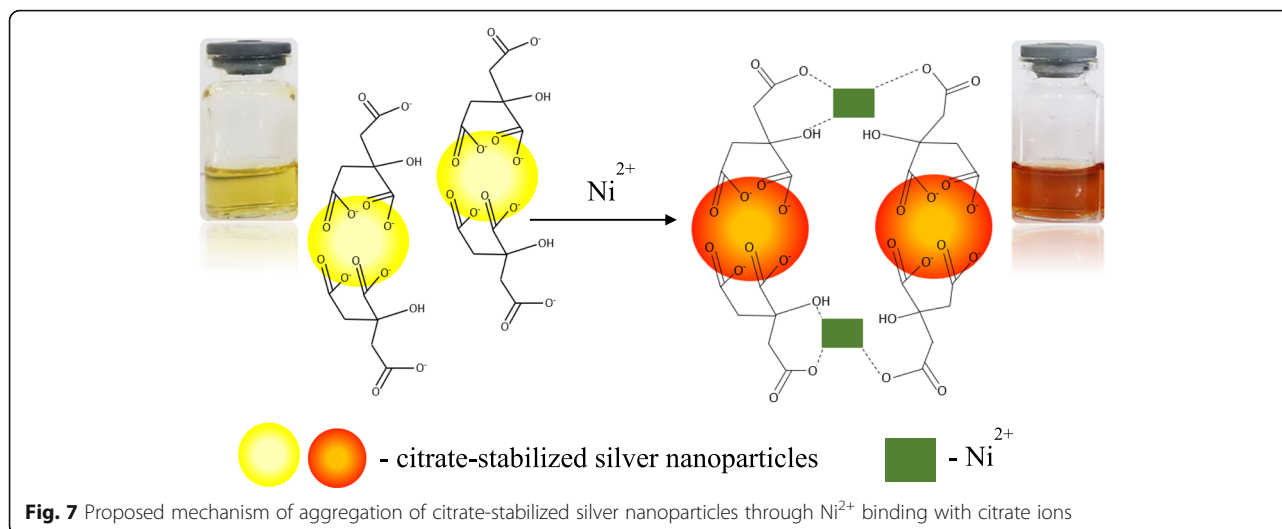
with its remaining free carboxyl and hydroxyl group. The metal binding process occurs on the surface of all the silver nanoparticles resulting in a decrease in inter-particle distance and a change in the morphology of the nanoparticles from a dispersed state to an aggregated state. This proposed mechanism is presented in Fig. 7.

The aggregation of the citrate-stabilized silver nanoparticles causes a visible color change in the solution attributed to the localized surface plasmon resonance of silver nanoparticles which is heavily dependent on particle morphology. When the silver nanoparticles change in state from dispersed state to an aggregated state, the absorbance behaviour of the solution changes and consequently its color.

#### Calibration curve

A calibration curve aids in quantitatively determining the amount of target analyte detected by the assay. In this case, the calibration curve was generated as a plot of absorbance ratio ( $A_{510}/A_{392}$ ) versus concentration. A





strong linear relationship was observed for  $\text{Ni}^{2+}$  concentration from 0.7 to 1.6 mM with a calibration equation  $y = 0.9702x + 0.6054$  and a coefficient of determination of 0.9958.

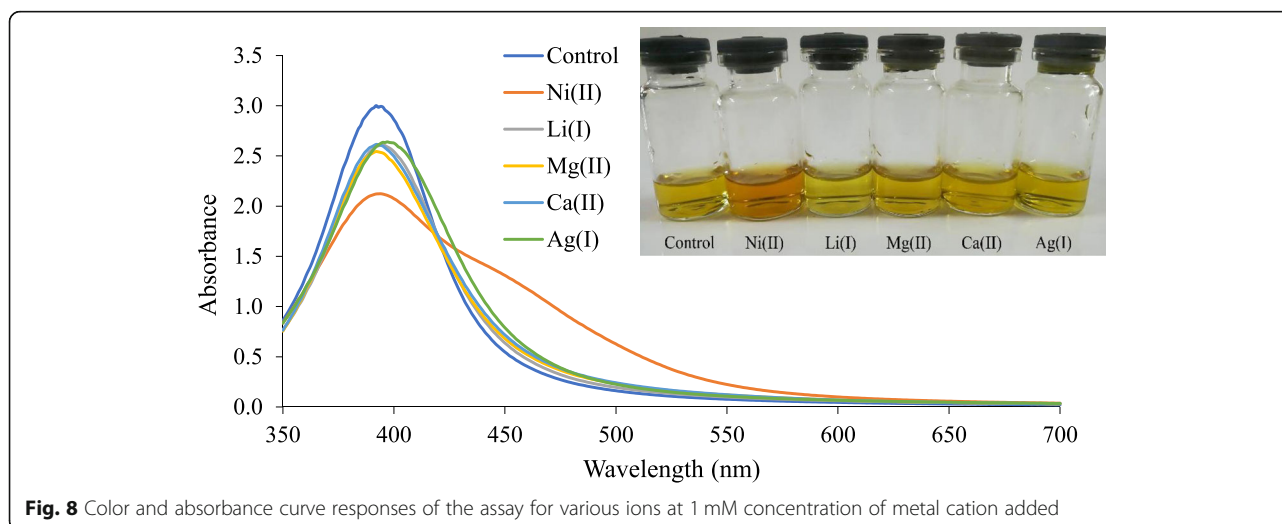
The limits of detection and quantification were also determined using the linear regression method suggested by Sanagi et al. [13]. The limits of detection and quantification are 0.75 and 1.52 mM, respectively.

#### Assay selectivity for nickel

In order to ensure assay preference for detecting  $\text{Ni}^{2+}$  ions in possible real water application, a selectivity study was conducted. The selectivity of the assay for  $\text{Ni}^{2+}$  was investigated by testing the color response and the absorbance ratio ( $A_{510}/A_{392}$ ) response of the citrate-stabilized silver nanoparticles to different common ions. Metals used were representative of the different groups such as  $\text{Li}^+$  for alkali metals,  $\text{Mg}^{2+}$  and  $\text{Ca}^{2+}$  for alkaline

earth metals and for hard water interference examination, and  $\text{Ag}^+$  for transition metals. The  $\text{Ni}^{2+}$  concentration used for the selectivity test was 1 mM. As observed in Fig. 8, only  $\text{Ni}^{2+}$  induced an observable color change from yellow to orange that is distinguishable to the naked eye. Other solutions remained bright yellow in color suggesting that no aggregation took place. This confirms that visually, the assay has excellent preference for  $\text{Ni}^{2+}$  over other representative metals. Their individual absorbance curve responses were consistent with the visual observation.

To further investigate and quantify the selectivity of the silver nanoparticle assay to  $\text{Ni}^{2+}$ , the resulting absorbance ratio ( $A_{510}/A_{392}$ ) of the solution upon interaction with the metal ions were treated as responses. The percent response for each metal ion was obtained by setting the response ( $A_{510}/A_{392}$ ) for  $\text{Ni}^{2+}$  at 100%. As shown in Fig. 9, all the other metal ions





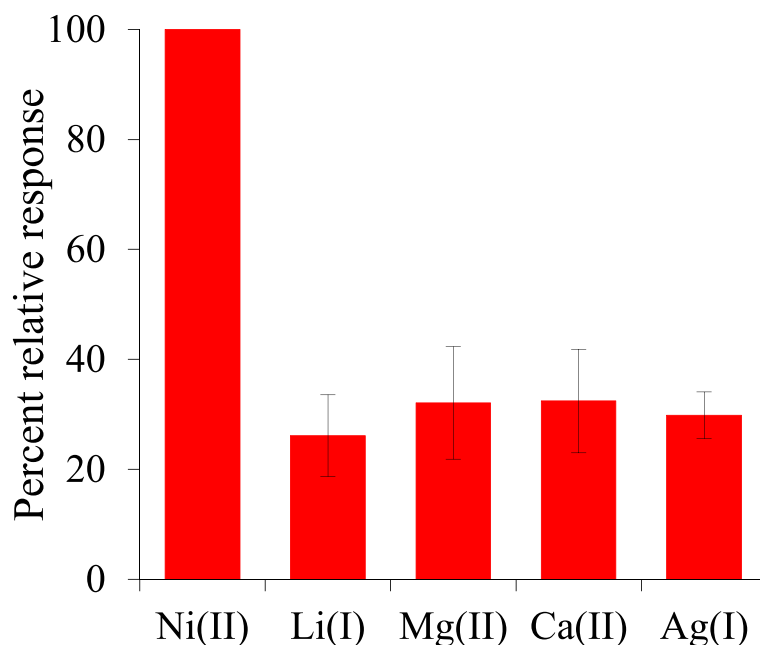


**Fig. 9** Relative responses of metal ions of less than 35% indicating assay preference for  $\text{Ni}^{2+}$

produced a significantly lower response of less than 35%.

Based on color, absorbance behavior and relative response, the results suggest that the assay can be used in real water to detect  $\text{Ni}^{2+}$  with minimal interference from the various representative metal ions.

#### Practical application: $\text{Ni}^{2+}$ sensing in tap water

To test the practicability of the citrate-stabilized silver nanoparticles in detecting  $\text{Ni}^{2+}$  in real water samples, the assay was applied to determine the heavy metal using the tap water collected from the School of Technology, University of the Philippines Visayas in Iloilo, Philippines.  $\text{Ni}^{2+}$  solutions of varying concentrations were prepared using tap water. Figure 10 shows the comparison of the color response of the assay in detecting  $\text{Ni}^{2+}$  in distilled water and in tap water.

The respective changes in the nanoparticle solution with the addition of distilled water and tap water containing  $\text{Ni}^{2+}$  showed slight differences in color. The

nanoparticle solution mixed with tap water containing  $\text{Ni}^{2+}$  produced deeper orange color when compared to the nanoparticle solution mixed with distilled water containing  $\text{Ni}^{2+}$ . The concentrations of  $\text{Ni}^{2+}$  detected by the assay from the tap water and distilled water, were calculated using the calibration equation generated previously. The calculated values are tabulated in Table 1.

The detected  $\text{Ni}^{2+}$  concentration in distilled water is in excellent agreement with the prepared concentrations. For tap water, the assay returned modest values with an average of 16% difference. The slight interference can be due to the presence of organic matter and combined effects of other ions present in the tap water. Overall, the results show the potential of citrate-stabilized silver nanoparticles as colorimetric sensor for detecting  $\text{Ni}^{2+}$  in tap water.

#### Conclusions

The potential of using citrate-stabilized silver nanoparticles for  $\text{Ni}^{2+}$  detection was investigated. Small, spherical,



**Fig. 10** Silver nanoparticle solution upon addition of (a) 1.1 mM, (b) 1.2 mM, and (c) 1.6 mM of  $\text{Ni}^{2+}$  in distilled water (DI) and tap water

**Table 1** Concentrations of Ni<sup>2+</sup> detected in distilled water and tap water (n = 3)

Prepared concentration (mM)	Detected in distilled water (mM)	Detected in tap water (mM)
1.1	1.1	1.3
1.2	1.2	1.4
1.6	1.6	1.4

monodispersed, and stable silver nanoparticles were produced using sodium borohydride as reducing agent and trisodium citrate as capping agent. The addition of increasing concentrations of Ni<sup>2+</sup> to the nanoparticle solution caused the nanoparticles to aggregate, resulting in changes in color and absorbance curve in the solution. A calibration curve was generated for Ni<sup>2+</sup> concentrations from 0.7 to 1.6 mM. A strong linearity was observed supported by a coefficient of determination of 0.9958. The limits of detection and quantification were determined to be 0.75 and 1.52 mM, respectively. In the test for real water applicability, the assay showed excellent preference for Ni<sup>2+</sup> over other metal ions tested as shown in the color, absorbance curve and relative response results. Furthermore, the assay was proven to be capable of detecting Ni<sup>2+</sup> in tap water samples.

#### Acknowledgements

The authors wish to thank the School of Technology, University of the Philippines Visayas (UPV) and the Nanotechnology Research Laboratory, Department of Chemical Engineering, University of the Philippines Diliman for the valuable resources extended to the authors during the conduct of the experiments. The authors also wish to thank the funding assistance of UPV through the Small Budget In-house Research Grant. The authors also acknowledge Mr. Adolfo Arthuraphael James L. Salise for his contributions to the study.

#### Authors' contributions

FEA conceptualized and secured funding for the study. All authors contributed to the data gathering, writing and analysis. All authors read and approved the final manuscript.

#### Funding

This work was supported by the University of the Philippines Visayas through the Small Budget In-House Research Grant.

#### Availability of data and materials

All data generated or analyzed during this study are available from the corresponding author on reasonable request.

#### Competing interests

The authors declare they have no competing interests.

Received: 8 May 2019 Accepted: 12 August 2019

Published online: 23 August 2019

#### References

- Nakajima K, Nansai K, Matsubae K, Tomita M, Takayanagi W, Nagasaka T. Global land-use change hidden behind nickel consumption. *Sci Total Environ*. 2017;586:730–7.
- Jaishankar M, Tseten T, Anbalagan N, Mathew BB, Beeregowda KN. Toxicity, mechanism and health effects of some heavy metals. *Interdiscip Toxicol*. 2014;7:60–72.
- Helaluddin ABM, Khalid RS, Alaama M, Abbas SA. Main analytical techniques used for elemental analysis in various matrices. *Trop J Pharm Res*. 2016;15:427–34.
- Lee S, Nam YS, Lee HJ, Lee Y, Lee KB. Highly selective colorimetric detection of Zn(II) ions using label-free silver nanoparticles. *Sensor Actuat B-Chem*. 2016;237:643–51.
- Vilela D, Gonzalez MC, Escarpa A. Sensing colorimetric approaches based on gold and silver nanoparticles aggregation: chemical creativity behind the assay. A review. *Anal Chim Acta*. 2012;751:24–43.
- Nsengiyuma G, Hu R, Li J, Li HB, Tian DM. Self-assembly of 1,3-alternate calix[4]arene carboxyl acids-modified silver nanoparticles for colorimetric Cu<sup>2+</sup> sensing. *Sensor Actuat B-Chem*. 2016;236:675–81.
- Shrivastava K, Sahu S, Patra GK, Jaiswal NK, Shankar R. Localized surface plasmon resonance of silver nanoparticles for sensitive colorimetric detection of chromium in surface water, industrial waste water and vegetable samples. *Anal Methods-UK*. 2016;8:2088–96.
- He Y, Zhang XH. Ultrasensitive colorimetric detection of manganese(II) ions based on anti-aggregation of unmodified silver nanoparticles. *Sensor Actuat B-Chem*. 2016;222:320–4.
- Jarujamrus P, Amatongchai M, Thima A, Khongrangdee T, Mongkontong C. Selective colorimetric sensors based on the monitoring of an unmodified silver nanoparticles (AgNPs) reduction for a simple and rapid determination of mercury. *Spectrochim Acta A*. 2015;142:86–93.
- Li HB, Cui ZM, Han CP. Glutathione-stabilized silver nanoparticles as colorimetric sensor for Ni<sup>2+</sup> ion. *Sensor Actuat B-Chem*. 2009;143:87–92.
- Shang Y, Wu FY, Qi L. Highly selective colorimetric assay for nickel ion using N-acetyl-L-cysteine-functionalized silver nanoparticles. *J Nanopart Res*. 2012;14:1169.
- Creighton JA, Blatchford CG, Albrecht MG. Plasma resonance enhancement of Raman scattering by pyridine adsorbed on silver or gold sol particles of size comparable to the excitation wavelength. *J Chem Soc Farad T 2*. 1979;75:790–8.
- Sanagi MM, Ling SL, Nasir Z, Hermawan D, Ibrahim WAW, Abu Naim A. Comparison of signal-to-noise, blank determination, and linear regression methods for the estimation of detection and quantification limits for volatile organic compounds by gas chromatography. *J AOAC Int*. 2009;92:1833–8.
- Paramelle D, Sadovoy A, Gorelik S, Free P, Hobley J, Fernig DG. A rapid method to estimate the concentration of citrate capped silver nanoparticles from UV-visible light spectra. *Analyst*. 2014;139:4855–61.
- Alula MT, Karamchand L, Hendricks NR, Blackburn JM. Citrate-capped silver nanoparticles as a probe for sensitive and selective colorimetric and spectrophotometric sensing of creatinine in human urine. *Anal Chim Acta*. 2018;1007:40–9.
- Solomon SD, Bahadory M, Jeyarajasingam AV, Rutkowsky SA, Boritz C, Mulfinger L. Synthesis and study of silver nanoparticles. *J Chem Educ*. 2007;84:322–5.
- Abou El-Nour KMM, Eftaiha A, Al-Warthan A, Ammar RAA. Synthesis and applications of silver nanoparticles. *Arab J Chem*. 2010;3:135–40.
- Terenteva EA, Apyari VV, Kochuk EV, Dmitrienko SG, Zolotov YA. Use of silver nanoparticles in spectrophotometry. *J Anal Chem*. 2017;72:1138–54.
- Roh J, Umh HN, Sim J, Park S, Yi J, Kim Y. Dispersion stability of citrate- and PVP-AgNPs in biological media for cytotoxicity test. *Korean J Chem Eng*. 2013;30:671–4.
- Munro CH, Smith WE, Garner M, Clarkson J, White PC. Characterization of the surface of a citrate-reduced colloid optimized for use as a substrate for surface-enhanced resonance Raman scattering. *Langmuir*. 1995;11:3712–20.
- Wyrzykowski D, Chmurzynski L. Thermodynamics of citrate complexation with Mn<sup>2+</sup>, Co<sup>2+</sup>, Ni<sup>2+</sup> and Zn<sup>2+</sup> ions. *J Therm Anal Calorim*. 2010;102:61–4.

#### Publisher's Note

Springer Nature remains neutral with regard to jurisdictional claims in published maps and institutional affiliations.